Thermodynamics of Glaciers

McCarthy Summer School 2014

Andy Aschwanden
University of Alaska Fairbanks, USA

August 2014

Note: This script is largely based on the *Physics of Glaciers I* lecture notes by Martin Lüthi and Martin Funk, ETH Zurich, Switzerland, with additions from *Greve and Blatter* (2009), *Gusmeroli et al.* (2010) and *Aschwanden et al.* (2012).

Glaciers are divided into three categories, depending on their thermal structure

Cold The temperature of the ice is below the pressure melting temperature throughout the glacier, except for maybe a thin surface layer.

Temperate The whole glacier is at the pressure melting temperature, except for seasonal freezing of the surface layer.

Polythermal Some parts of the glacier are cold, some temperate. Usually the highest accumulation area, as well as the upper part of an ice column are cold, whereas the surface and the base are at melting temperature.

The knowledge of the distribution of temperature in glaciers and ice sheets is of high practical interest

- A temperature profile from a cold glacier contains information on past climate conditions.
- Ice deformation is strongly dependent on temperature (temperature dependence of the rate factor A in Glen's flow law).
- The routing of meltwater through a glacier is affected by ice temperature. Cold ice is essentially impermeable, except for discrete cracks and channels.
- If the temperature at the ice-bed contact is at the pressure melting temperature the glacier can slide over the base.

- Wave velocities of radio and seismic signals are temperature dependent. This affects the interpretation of ice depth soundings.

The distribution of temperature in a glacier depends on many factors. Heat sources are on the glacier surface, at the glacier base and within the body of the ice. Heat is transported through a glacier by conduction (diffusion), is advected with the moving ice, and is convected with water or air flowing through cracks and channels. Heat sources within the ice body are (Figure 2)

- dissipative heat production (internal friction) due to ice deformation,
- frictional heating at the glacier base (basal motion)
- frictional heating of flowing water at englacial channel walls,
- release or consumption of (latent) heat due to freezing and melting.

The importance of the processes depends on the climate regime a glacier is subjected to, and also varies between different parts of the same glacier.

1 Energy balance equation

The energy balance equation for internal energy U is an advection-diffusion-production equation which in a spatially fixed (Eulerian) reference frame is given by

$$\rho \left(\frac{\partial U}{\partial t} + \underbrace{\mathbf{v} \cdot \nabla U}_{\text{advection}} \right) = - \underbrace{\nabla \cdot \mathbf{q}}_{\text{diffusion}} + \underbrace{Q}_{\text{production}} , \tag{1}$$

where ρ is density and q is a non-advective energy flux. Note that, strictly speaking, internal energy is not a conserved quantity, only the sum of internal energy and kinetic energy is conserved.

2 Cold ice

If ice is below the pressure melting point, we can replace internal energy $U = cT$ with temperature T:

$$\rho c \left(\frac{\partial T}{\partial t} + \underbrace{\mathbf{v} \cdot \nabla T}_{\text{advection}} \right) = \underbrace{\nabla k \nabla T}_{\text{diffusion}} + \underbrace{Q}_{\text{production}} , \tag{2}$$

where specific heat capacity c and thermal conductivity k are given in Table 1. In general, specific heat capacity and thermal heat conductivity are functions of temperature (e.g. *Ritz*, 1987),

$$c(T) = (146.3 + 7.253T[\mathrm{K}])\,\mathrm{J\,kg^{-1}\,K^{-1}} \tag{3}$$

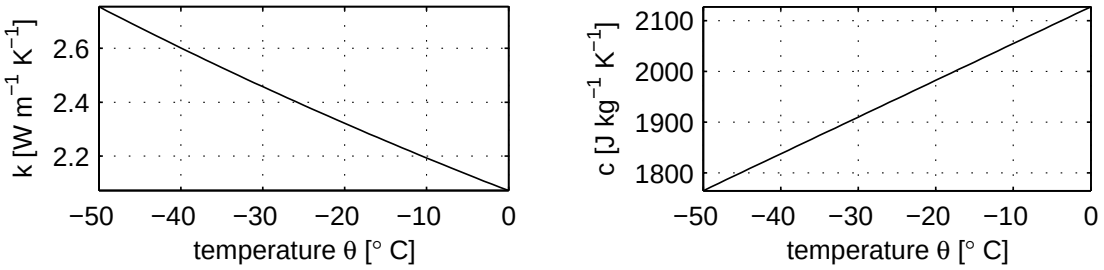

Figure 1: Heat conductivity k (left) and specific heat c (right) for the temperature range from $-50°$ C until $0°$ C. After *Ritz* (1987).

and

$$k(T) = 9.828e^{-0.0057T[\mathrm{K}]}\,\mathrm{W\,m^{-1}\,K^{-1}}. \tag{4}$$

For constant thermal conductivity k and in one dimension (the vertical direction z and vertical velocity w) the energy balance equation (2) reduces to

$$\rho\, c \left(\frac{\partial T}{\partial t} + w \frac{\partial T}{\partial z} \right) = k\, \frac{\partial^2 T}{\partial z^2} + P. \tag{5}$$

The heat production (source term) P can be due to different processes (see Figure 2):

Dissipation In viscous flow the *dissipation* due to ice deformation (heat release due to internal friction, often called strain heating) is $P = \mathrm{tr}(\dot{\boldsymbol{\varepsilon}}\boldsymbol{\sigma}) = \dot{\varepsilon}_{ij}\sigma_{ji}$, where $\dot{\boldsymbol{\varepsilon}}$ and $\boldsymbol{\sigma}$ are the strain rate tensor and the stress tensor, respectively.. Because usually the shearing deformation dominates glacier flow

$$P_{\mathrm{def}} \simeq 2\, \dot{\varepsilon}_{xz}\sigma_{xz}\,.$$

Sliding friction The heat production is the rate of loss of potential energy as an ice column of thickness H moves down slope. If all the frictional energy is released at the bed due to sliding with basal velocity u_b,

$$P_{\mathrm{friction}} = \tau_b u_b \sim \rho g H \tan\beta\, u_b\,,$$

where τ_b is basal shear stress and β is the bed inclination.

Refreezing of meltwater Consider ice that contains a volume fraction ω of water. If a freezing front is moving with a velocity v_{freeze} relative to the ice, the rate of latent heat production per unit area of the freezing front is

$$P_{\mathrm{freeze}} = v_{\mathrm{freeze}}\, \omega \rho_w L.$$

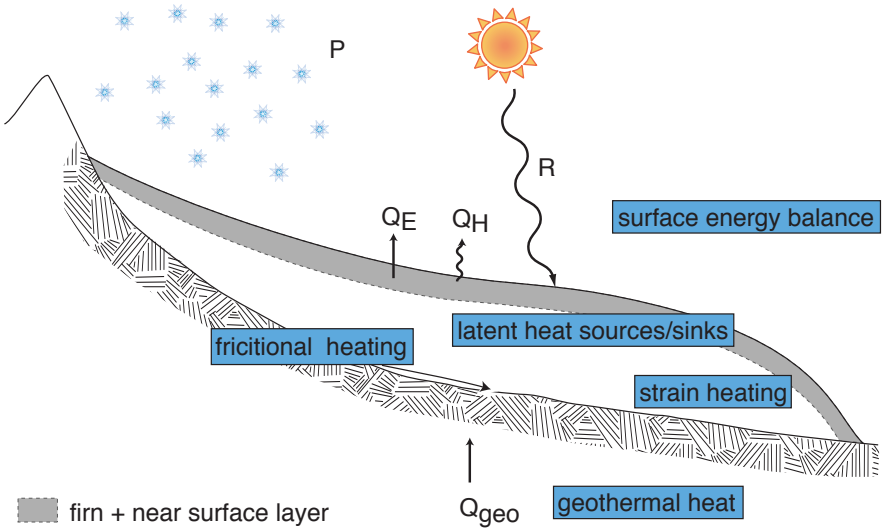

Figure 2: Sources for heat production

2.1 Steady temperature profile

The simplest case is a vertical steady state temperature profile (Eq. 5 without time derivative) in stagnant ice ($w = 0$) without any heat sources ($P = 0$), and with constant thermal conductivity k. The heat flow equation (5) then reduces to the diffusion equation

$$\frac{\partial^2 T}{\partial z^2} = 0. \tag{6}$$

Integration with respect to z gives

$$\frac{dT}{dz} = Q := kG \tag{7}$$

Quantity	Symbol	Value	Unit
$\mathrm{kg\,m^{-3}}$			
Specific heat capacity of water	c_w	4182	$\mathrm{J\,K^{-1}\,kg^{-1}}$
Specific heat capacity of ice	c_i	2093	$\mathrm{J\,K^{-1}\,kg^{-1}}$
Thermal conductivity of ice (at 0° C)	k	2.1	$\mathrm{W\,m^{-1}\,K^{-1}}$
Thermal diffusivity of ice (at 0° C)	κ	$1.09 \cdot 10^{-6}$	$\mathrm{m^2\,s^{-1}}$
Latent heat of fusion (ice/water)	L	333.5	$\mathrm{kJ\,kg^{-1}}$
Depression of melting temperature (Clausius-Clapeyron constant)			
- pure ice and air-free water	γ	0.0742	$\mathrm{K\,MPa^{-1}}$
- pure ice and air-saturated water	γ	0.098	$\mathrm{K\,MPa^{-1}}$

Table 1: Thermal properties of ice and water.

where $G = \nabla T$ is the (constant) temperature gradient. Integrating again leads to

$$T(z) = Gz + T(0) = \frac{Q}{k}z + T(0). \tag{8}$$

Ice temperature changes linearly with depth. Choosing for example a temperature gradient of $G = 1\,\mathrm{K}/100\,\mathrm{m} = 0.01\,\mathrm{K\,m^{-1}} = 10\,\mathrm{mK\,m^{-1}}$ gives a heat flux of $Q = kG = 0.021\,\mathrm{W\,m^{-2}} = 21\,\mathrm{mW\,m^{-2}}$. For comparison, typical geothermal fluxes are $40 - 120\,\mathrm{mW\,m^{-2}}$.

To transport a geothermal flux of $80\,\mathrm{mW\,m^{-2}}$ through a glacier of 200 m thickness, the surface temperature has to be 8 K lower than the temperature at the glacier base.

The above calculations (partly) explain why there can be water at the base of the Greenland and Antarctic ice sheets. Under an ice cover of 3000 m and at surface temperatures of $-50°\,\mathrm{C}$ (in Antarctica), only a heat flux of $Q = k \cdot 50\,\mathrm{K}/3000\,\mathrm{m} = 35\,\mathrm{mW\,m^{-2}}$ can be transported away. Notice that horizontal and vertical advection change this result considerably.

2.2 Ice temperature close to the glacier surface

The top 15 m of a glacier (near surface layer, Figure 2) are subject to seasonal variations of temperature. In this part of the glacier *heat flow* (*heat diffusion*) is dominant. If we neglect advection we can rewrite Equation (5) to obtain the well known *Fourier law* of heat diffusion

$$\frac{\partial T}{\partial t} = \kappa \frac{\partial^2 T}{\partial h^2} \tag{9}$$

where h is depth below the surface, and $\kappa = k/(\rho C)$ is the *thermal diffusivity* of ice. To calculate a temperature profile and changes with time we need boundary conditions. Periodically changing boundary conditions at the surface such as day/night and winter/summer can be approximated with a sine function. At depth we assume a constant temperature T_0

$$\begin{aligned} T(0,t) &= T_0 + \Delta T_0 \cdot \sin(\omega t)\,, \\ T(\infty,t) &= T_0\,. \end{aligned} \tag{10}$$

T_0 is the mean surface temperature and ΔT_0 is the amplitude of the periodic changes of the surface temperature. The duration of a period is $2\pi/\omega$. The solution of Equation (9) with the boundary condition (10) is

$$T(h,t) = T_0 + \Delta T_0 \exp\left(-h\sqrt{\frac{\omega}{2\kappa}}\right) \sin\left(\omega t - h\sqrt{\frac{\omega}{2\kappa}}\right). \tag{11}$$

The solution is plotted for realistic values of T_0 and ΔT on Colle Gnifetti (4550 m a.s.l., Monte Rosa, Valais). Notice that full ice density has been assumed for the plot, instead of

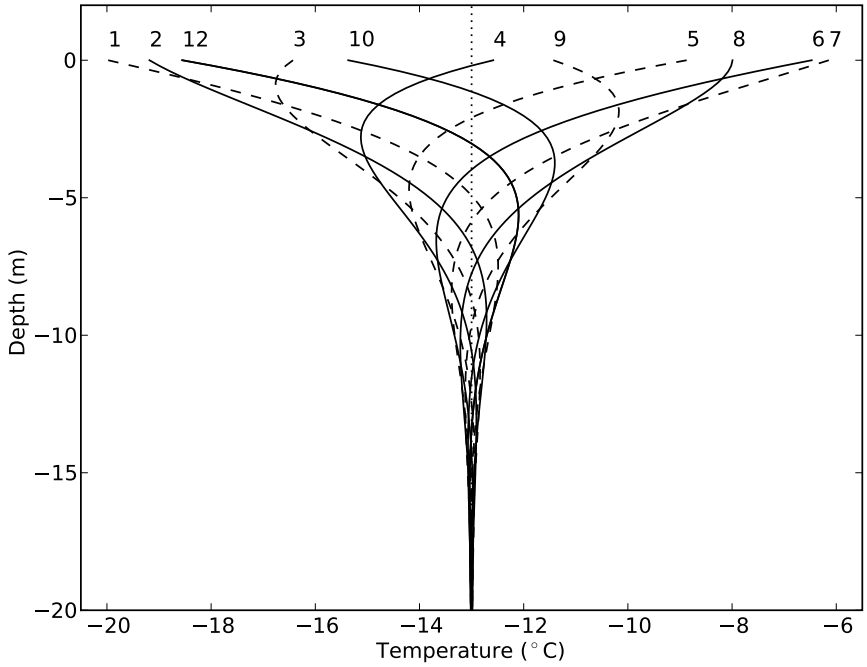

Figure 3: Variation of temperature with depth for the conditions at Colle Gnifetti. Numbers next to curves indicate months (1 corresponds to January).

a firn layer with strongly changing thermal properties, and vertical advection is neglected.

The solution (Eq. 11) has some noteworthy properties

a) The amplitude varies with depth h as

$$\Delta T(h) = \Delta T_0 \exp\left(-h\sqrt{\frac{\omega}{2\kappa}}\right) \tag{12}$$

b) The temperature $T(h,t)$ has an extremum when

$$\sin\left(\omega t - h\sqrt{\frac{\omega}{2\kappa}}\right) = \pm 1 \qquad \Rightarrow \qquad \omega t - h\sqrt{\frac{\omega}{2\kappa}} = \frac{\pi}{2}$$

and therefore

$$t_{\max} = \frac{1}{\omega}\left(\frac{\pi}{2} + h\sqrt{\frac{\omega}{2\kappa}}\right) \tag{13}$$

The phase shift is increasing with depth below the surface.

c) The heat flux $G(h,t)$ in a certain depth h below the surface is

$$G(h,t) = -k\frac{\partial T}{\partial h} = \quad \text{(complicated formula that is easy to derive)}$$

For the heat flux $G(0,t)$ at the glacier surface we get

$$G(0,t) = \Delta T_0 \sqrt{\omega \rho\, c\, k}\, \sin\left(\omega t + \frac{\pi}{4}\right)$$

$G(0,t)$ is maximal when

$$\sin\left(\omega t + \frac{\pi}{4}\right) = 1 \qquad \Rightarrow \qquad \omega t + \frac{\pi}{4} = \frac{\pi}{2} \qquad \Longrightarrow \qquad t_{\max} = \frac{\pi}{4\omega}$$

where $t_{\max}$ is the time when the heat flux at the glacier surface is maximum.

Temperature:	$t_{\max} = \dfrac{\pi}{2\omega}$
Heat flux:	$t_{\max} = \dfrac{\pi}{4\omega}$

The difference is $\pi/(4\omega)$ and thus 1/8 of the period. The maximum heat flux at the glacier surface is 1/8 of the period ahead of the maximum temperature. For a yearly cycle this corresponds to 1.5 months.

d) From the ratio between the amplitudes in two different depths the heat diffusivity κ can be calculated

$$\frac{\Delta T_2}{\Delta T_1} = \exp\left((h_1 - h_2)\sqrt{\frac{\omega}{2\kappa}}\right) \qquad \Longrightarrow \qquad \kappa = \frac{\omega}{2}\left(\frac{h_2 - h_1}{\ln\frac{\Delta T_2}{\Delta T_1}}\right)^2$$

There are, however, some restrictions to the idealized picture given above

- The surface layers are often not homogeneous. In the accumulation area density is increasing with depth. Conductivity k and diffusivity κ are functions of density (and also temperature).
- In nature the surface boundary condition is not a perfect sine function.
- The ice is moving. Heat diffusion is only one part, heat advection may be equally important.
- Percolating and refreezing melt water can drastically change the picture by providing a source of latent heat (see below).

Superimposed on the yearly cycle are long term temperature changes at the glacier surface. These penetrate much deeper into the ice, as can be seen from Equation (12), since ω decreases for increasing forcing periods.

In spring or in high accumulation areas the surface layer of a glacier consists of snow or firn. If surface melting takes place, the water percolates into the snow or firn pack and freezes when it reaches a cold layer. The freezing of 1 g of water releases sufficient heat to raise the temperature of 160 g of snow by 1 K. This process is important to "annihilate" the winter cold from the snow or firn cover in spring, and is the most important process altering the thermal structure of high accumulation areas and of the polar ice sheets.

2.3 Advection – diffusion

Close to the ice divides in the central parts of an ice sheet, the ice velocity is mainly vertical down. Under the assumptions of only vertical advection, no heat generation, and a frozen base we can calculate the steady state temperature profile with the simplified Equation (5)

$$\kappa \frac{d^2T}{dz^2} = w(z) \frac{dT}{dz} \tag{14}$$

The boundary conditions are

$$\begin{array}{lll} \text{surface:} & z = H: & \text{temperature } T_s = \text{const} \\ \text{bedrock:} & z = 0: & \text{heat flux } -k \left(\frac{dT}{dz}\right)_B = G = \text{const} \end{array}$$

For the first integration we substitute $f = \frac{dT}{dz}$ so that $\kappa f' = wf \implies \frac{f'}{f} = \frac{1}{\kappa} w$ with the solution

$$\frac{dT(z)}{dz} = \left(\frac{dT}{dz}\right)_B \exp\left(\frac{1}{\kappa} \int_0^z w(z)\, dz\right). \tag{15}$$

Now we make the assumption that the vertical velocity is $w(z) = -bz/H$, with the vertical velocity at the surface equal to the net mass balance rate $w_s = -\dot{b}$. With the definition $l^2 := 2\kappa H/\dot{b}$ we get

$$T(z) - T(0) = \left(\frac{dT}{dz}\right)_B \int_0^z \exp\left(-\frac{z^2}{l^2}\right) dz \tag{16}$$

which has the solution

$$T(z) - T_s = \frac{\sqrt{\pi}}{2} l \left(\frac{dT}{dz}\right)_B \left[\operatorname{erf}\left(\frac{z}{l}\right) - \operatorname{erf}\left(\frac{H}{l}\right)\right] . \tag{17}$$

The so-called *error function* is tabulated and implemented in any mathematical software (usually as `erf`), and is defined as

$$\operatorname{erf}(x) = \frac{2}{\sqrt{\pi}} \int_0^x \exp(-x^2)\, dx.$$

We now introduce the useful definition of the *Péclet Number* $\mathrm{Pe} = wH/\kappa$ which is a measure of the relative importance of advection and diffusion. The shape of the temperature profiles in Figure 4 only depends on the Péclet Number. Depth and temperature can be scaled by the dimensionless variables

$$\begin{aligned} &\text{scaled distance above bed} && \xi = \frac{z}{H}\,, \\ &\text{scaled temperature} && \Theta = \frac{k(T - T_s)}{GH}\,. \end{aligned}$$

2.4 Cold glaciers

In cold glaciers heat flow is driven by temperature gradients. Usually the base is warmest due to dissipation, friction and geothermal heat. This has the consequence that heat is flowing from the base into the ice body, warming up the ice. Advection of warm or cold ice strongly influences local ice temperature. Cold glaciers exist in the McMurdo Dry Valleys in Antartica and at high altitudes at lower latitudes.

In the Alps, for example, cold glaciers were observed at altitudes above 3900 m a.s.l.. The most famous of these is Colle Gnifetti (4550 m a.s.l.), the highest accumulation basin of the Gorner-/Grenzgletscher system. At temperatures of about $-13°$ C the ice conserves atmospheric conditions such as impurities and air bubbles. Surface melting only takes place on exceptionally hot days and leads to formation of ice lenses. Many ice cores have been drilled on Colle Gnifetti and were investigated in the laboratory to obtain the climate history of central Europe.

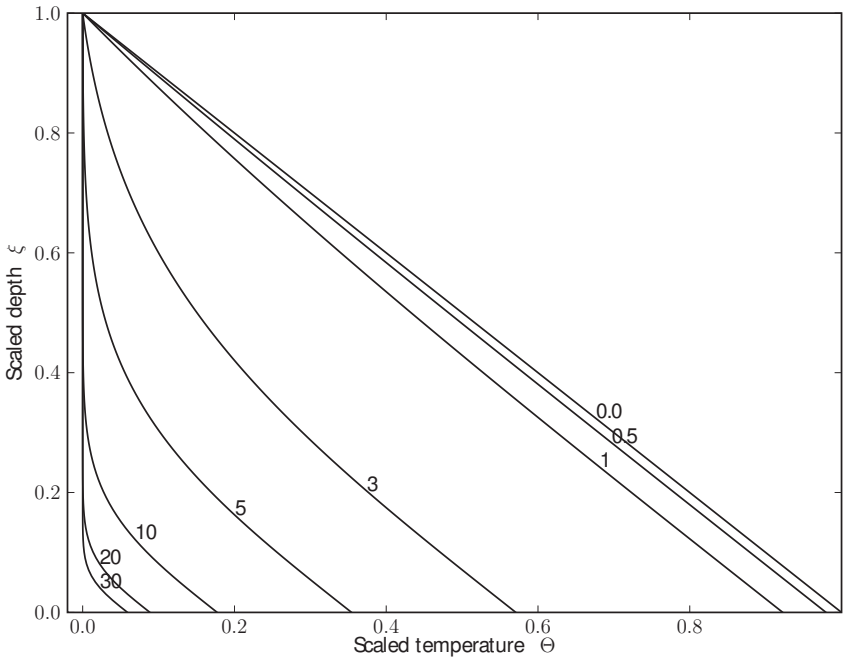

Figure 4: Dimensionless steady temperature profiles in terms of the dimensionless variables ξ and Θ for various values of the Péclet number Pe (next to curves).

Figure 5 shows two temperature profiles measured in boreholes 200 m apart on the same flow line on Colle Gnifetti. In the absence of advection and density gradients, one would expect straight steady state temperature profiles. The unequal curvature of the modeled steady state profiles (Fig. 5a) is due to firn density and different advection regimes. This shows that the interpretation of temperature profiles to deduce past climate can be quite tricky.

The marked bend towards warmer temperature at 30 m depth is due to changing surface temperatures. Numerical modeling showed that the temperature increase by 1° C around 1990 is mainly responsible for this feature (the profiles were measured in 1995/96; in 1982 the transient profiles looked like the steady state configuration).

Modeling the advection and conduction of heat in a glacier is usually not sufficient. The geothermal heat flux close to the glacier base is affected by the ice temperature, and therefore by the glacier flow, and the flux of meltwater. Figure 6 shows the temperature distribution in whole massif, with the glacier on top. Notice that there are areas within the mountain where heat flows horizontally (heat always flows perpendicular to the isotherms). Heat flux at sea level was assumed to be $70\,\mathrm{mW\,m^{-2}}$, but it had to be greatly reduced to match the observed fluxes. In the model this was accomplished with freezing/thawing ice within the rock (permafrost), which is a reaction to climate changes since the last ice age. The lowest calculated permafrost margin was at about 2900 m elevation.

3 Temperate ice

In temperate ice, the liquid water fraction ω, replaces u:

$$\rho L \left(\frac{\partial \omega}{\partial t} + \mathbf{v} \cdot \nabla \omega \right) = -\nabla \cdot \mathbf{q} + Q, \tag{18}$$

where L is latent heat of fusion, and u and ω are related by $u = \omega L$. Specifying the non-advective flux q is less straight-forward than for cold ice. Both Fick-type and Darcy-type diffusion closures haven been proposed. Generally it is assumed to be small, and often set to zero.

3.1 Temperate glaciers

Liquid water, generated from melting snow or direct input from rainfall, is routed down-glacier by supraglacial streams. When such streams intersect vertical shafts (moulins), crevasses or fractures, water can enter the macroscopic englacial water system (MWS, Figure 7a) mainly formed by a network of decimeter size, hydraulically connected fractures which can route macroscopic volumes of water to the bed of the glacier (*Fountain and Walder*, 1998; *Fountain et al.*, 2005).

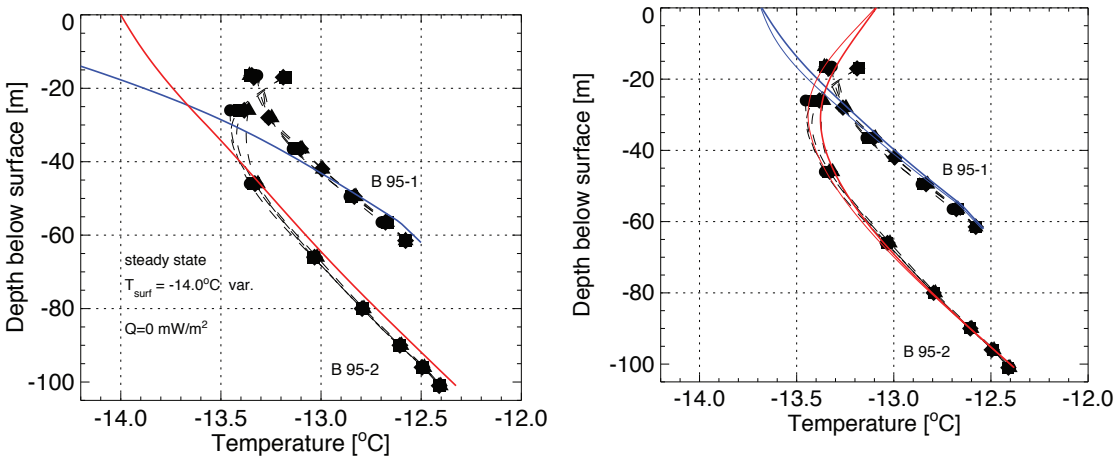

Figure 5: Markers indicate temperatures measured in two boreholes on the same flow line, 200 m apart, on Colle Gnifetti. Solid lines are the results of numerical interpretation of the data with steady state (left) and transient (right) temperature evolution. Notice that the different curvature of the steady state profiles is due to firn density and advection. From *Lüthi and Funk* (2001).

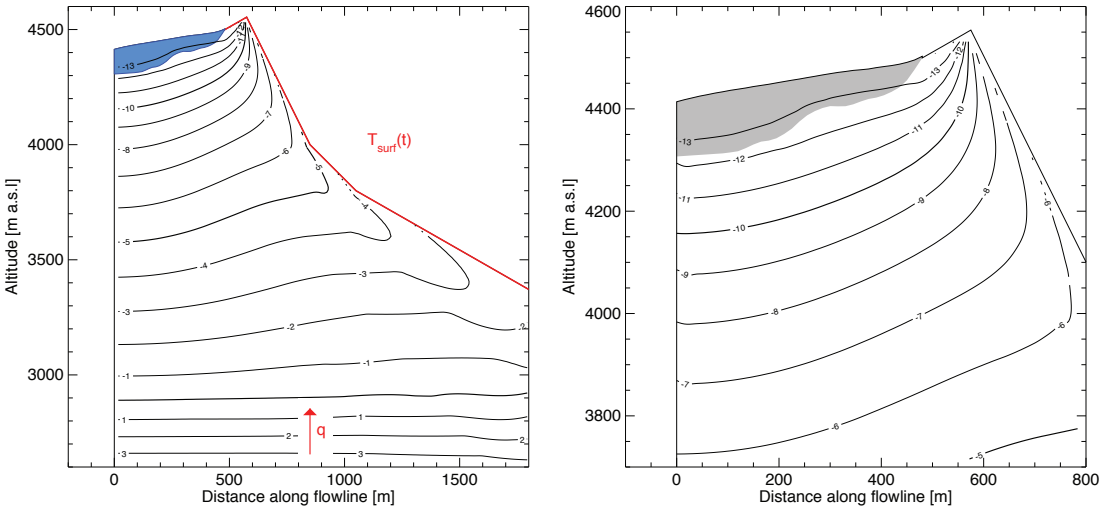

Figure 6: Modeled temperature distribution within the Monte Rosa massif. Notice the highly increased surface temperature on the south (right) face which leads to horizontal heat fluxes close to steep mountain faces. Thawing permafrost at the base of the mountain was essential to reproduce the measured heat flux at the glacier base. From *Lüthi and Funk* (2001).

Water in glaciers occurs also in a fundamentally different system unconnected from MWS: the microscopic water system (mWS, Figure 7b). mWS is formed by small (μm) water inclusions found in veins along three grain intersections, lenses on grain boundaries and in irregular shapes (*Raymond and Harrison*, 1975; *Nye*, 1989; *Mader*, 1992; *Fountain and Walder*, 1998). Such water inclusions are primarily generated in the accumulation area where meltwater percolates in the porous firn and become part of the glacier-ice crystalline structure when pores closed for compaction (*Paterson*, 1971; *Lliboutry*, 1976; *Pettersson et al.*, 2004).

In a temperate glacier, all heat that is produced at the boundaries or within the glacier is used to melt ice. This meltwater then becomes part of mWS. The water content, however, is small, usually between 0.1 and 4 volume percent. The water is stored in veins and triple junctions between the ice grains, where it can slowly percolate through the ice matrix if veins are not blocked by air bubbles. The water between ice grains has an important effect on the deformation properties of ice, and it affects the rate factor A in Glen's flow law (*Duval*, 1977; *Paterson*, 1994)

$$\begin{aligned} A(\omega) &= (3.2 + 5.8\omega) \cdot 10^{-15}\,\mathrm{kPa}^{-3}\,\mathrm{s}^{-1} \\ &= (101 + 183\omega)\,\mathrm{MPa}^{-3}\,\mathrm{a}^{-1}\,, \end{aligned} \tag{19}$$

where ω is the percentage of water within the ice (also called moisture content or liquid water fraction). Temperate glacier ice is a mixture of ice ($97-99\,\%$), water ($1-3\,\%$), and small amounts of air and minerals. For pure ice the melting temperature T_m depends on absolute pressure p by

$$T_m = T_{tp} - \gamma\,(p - p_{\mathrm{tp}})\,, \tag{20}$$

where $T_{tp} = 273.16\,\mathrm{K}$ and $p_{tp} = 611.73\,\mathrm{Pa}$ are the triple point temperature and pressure of water. The Clausius-Clapeyron constant is $\gamma_p = 7.42 \cdot 10^{-5}\,\mathrm{K\,kPa}^{-1}$ for pure water/ice. Since glacier ice is not pure, the value of γ can be as high as $\gamma_a = 9.8 \cdot 10^{-5}\,\mathrm{K\,kPa}^{-1}$ for air saturated water (*Harrison*, 1975).

4 Polythermal glaciers and ice sheets

Polythermal glaciers occur in different climates and at different geographic locations. Given the winter cooling of the surface layer in temperate glaciers, or the summer warming of the surface layer in cold glaciers, most glaciers are seasonally polythermal. The only exceptions are perhaps cold glaciers in the extremely cold climate of Antarctica. Considering only perennial polythermal glaciers, the most frequent structures are the so-called Scandinavian-type and Canadian-type polythermal glaciers (Figure 8).

The Scandinavian type occurs in Svalbard (*Bamber*, 1988; *Jania et al.*, 1996), Scandinavia (*Holmlund and Eriksson*, 1989), the Rocky Mountains (*Paterson*, 1971), Alaska and the Antarctic Peninsula (*Breuer et al.*, 2006). Such glaciers are mostly temperate except for a cold surface layer in the ablation zone. This seemingly paradoxical situation may be

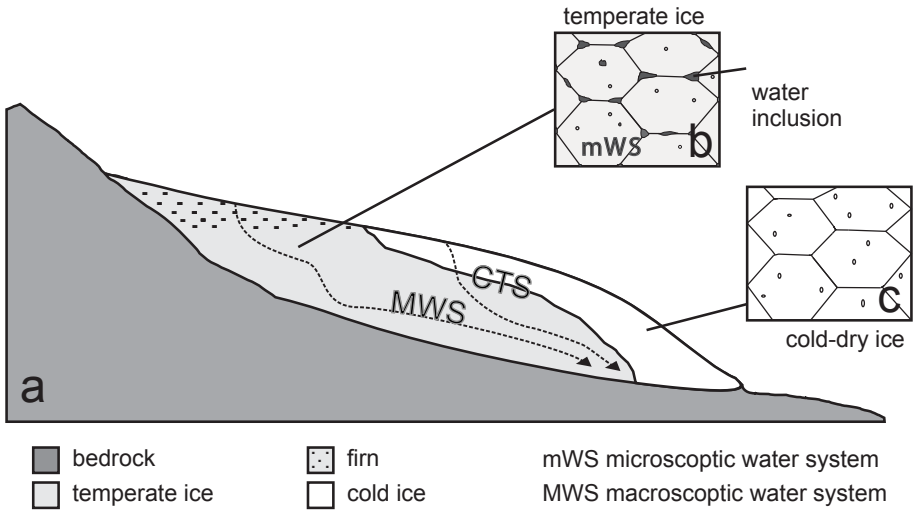

Figure 7: Illustration of macroscopic water system (MWS) and microscopic water system (mWS) found in the temperate ice. The cold-temperate transition surface (CTS) is the englacial boundary separating temperate ice (b) from the cold ice (c). Modified after *Gusmeroli et al.* (2010)

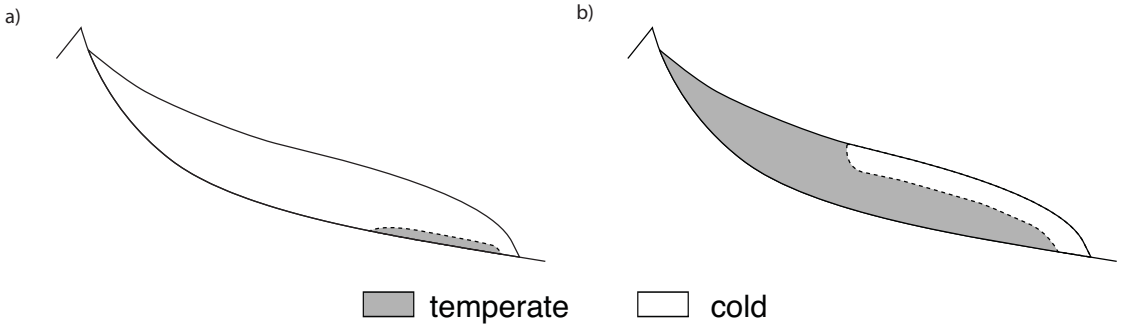

Figure 8: Longitudinal section of glaciers with (a) Canadian-type and (b) Scandinavian-type polythermal structures.

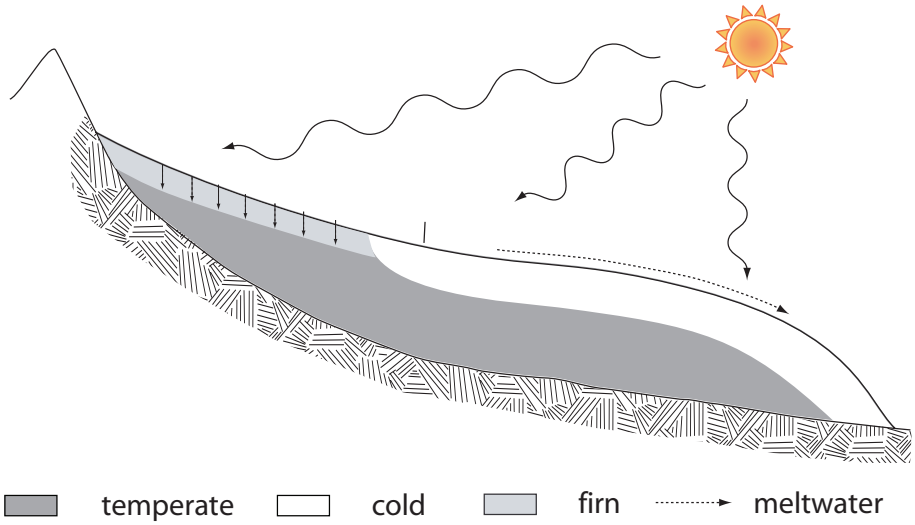

Figure 9: Scandinavian-type polythermal structure. Most of the ice is temperate (gray color) except for a cold near-surface layer in the ablation zone. The summer heat input is stored due to percolation of meltwater into the upper firn area, whereas this heat is lost due to runoff of meltwater over the impermeable surface ice in the ablation zone.

explained by the summer heat input, which is stored due to percolation of meltwater into the upper firn area, whereas this heat is lost due to runoff of meltwater over the impermeable surface ice in the ablation zone (Figure 9). If winter temperatures increase, the cold layer thins and may eventually disappear, leaving an entirely temperate glacier.

The Canadian type occurs at high Arctic latitudes in Canada (*Blatter*, 1987; *Blatter and Kappenberger*, 1988) and Alaska, but the large ice sheets in Greenland and Antarctica also show this polythermal structure locally. Canadian-type glaciers are mostly cold except for a temperate layer at the bed in the ablation zone. The temperate layer at the bedrock can be of considerable thickness and is due to geothermal heat flux and heat dissipation due to friction and ice deformation. The latter is highest close to the base because stresses and strain rates are highest there. Depending on the climate, ice thickness and ice flow, the thickness of this basal layer may shrink to zero, leaving a so-called basal hot spot (*Classen and Clarke*, 1971). There may be additional polythermal structures, such as combinations of the above if glaciers span an extreme altitude range, or at confluences of glaciers with different thermal structures (*Eisen et al.*, 2009).

Gorner-/Grenzgletscher is the biggest polythermal glacier in the Alps. Cold ice originating from Colle Gnifetti is advected down to the confluence area at 2500 m a.s.l., and all the way to the glacier tongue. Figure 10 shows the slow cooling of a borehole in the confluence area after hot-water drilling. The cold ice is mostly impermeable to water which leads to the formation of deeply incised river systems and surficial lakes which sometimes drain through crevasses or *moulins*.

Polythermal glaciers are usually cold in their core and temperate close to the surface

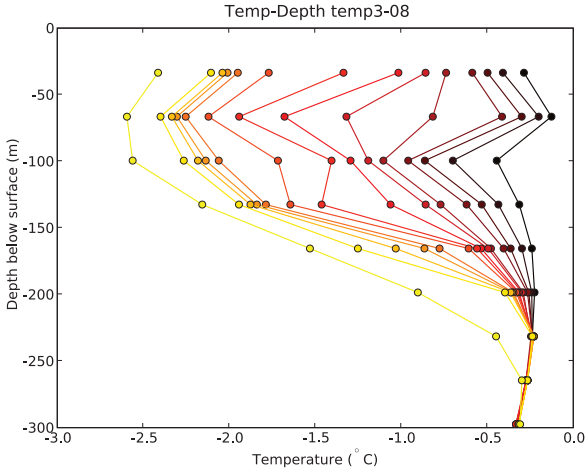

Figure 10: Cooling of a borehole drilled in the confluence area of Gorner-/Grenzgletscher. Temperatures measured every day after completion of drilling are shown in increasingly lighter colors, and after three months (leftmost yellow curve). Data from *Ryser* (2009).

and at the bedrock. Heat sources at the surface are from the air (sensible heat flux), direct solar radiation (short wave), thermal radiation (long wave), and the penetration and refreezing of melt water (convection and latent heat).

Nice examples of the polythermal structure of the Greenland ice sheet are the temperature profiles in Figure 11, measured in Jakobshavn Isbræ, Greenland (*Iken et al.*, 1993; *Funk et al.*, 1994; *Lüthi et al.*, 2002). The drill sites are located 50 km inland of the margin of the Greenland ice sheet, at a surface elevation is 1100 m a.s.l., where ice thickness on the ice sheet is 830 m, but about 2500 m in the ice stream center.

In Figure 11 (bottom left) temperatures are highest close to the surface and close to the bed. The thick, very cold layer in between is advected from the inland parts of the ice sheet (see Figure 12 top). The lowest 31 m are at the pressure melting temperature $T_m = -0.55°\,\mathrm{C}$. A quick calculation with Equation (20), and reasonable values for the ice density and gravity gives

$$\begin{aligned} T_m &= T_{tp} - \gamma_p(p - p_{\mathrm{tp}}) = T_p - \gamma_p(\rho g H - p_{tp}) \\ &= 273.16\,\mathrm{K} - 7.42 \cdot 10^{-5}\,\mathrm{K\,kPa^{-1}}\left(900\,\mathrm{kg\,m^3} \cdot 9.825\,\mathrm{m\,s^{-2}} \cdot 830\,\mathrm{m}\right) \\ &\simeq 273.16\,\mathrm{K} - 0.545\,\mathrm{K} \simeq 272.615\,\mathrm{K} = -0.54°\,\mathrm{C}\,. \end{aligned} \tag{21}$$

The strong curvature of the temperature profiles where they are coldest indicates that the ice is warming. Upward heat flux from the temperate zone close to the base is very high. The temperature gradient just above the CTS (800 m depth) in profile D is $0.048\,\mathrm{K\,m^{-1}}$. The upward heat flux therefore is (per unit area)

$$Q \;=\; k\,\frac{\partial T}{\partial z} \;\simeq\; 2.1\,\mathrm{W\,m^{-1}\,K^{-1}} \cdot 0.048\,\mathrm{K\,m^{-1}} \;\simeq\; 0.1\,\mathrm{W\,m^{-2}}\,. \tag{22}$$

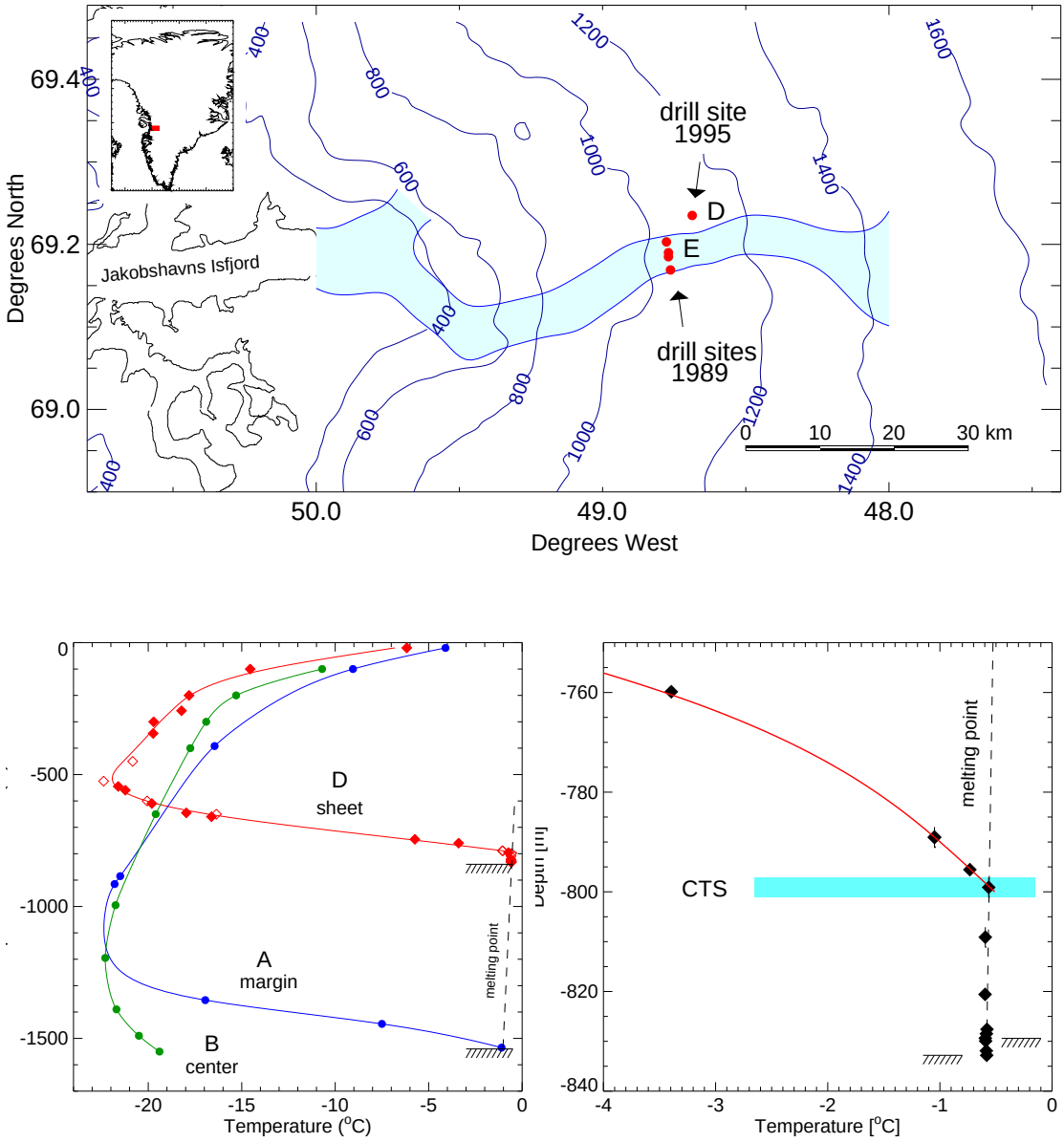

Figure 11: Top: Location map of the drill sites on Jakobshavn Isbræ, Greenland, where temperature profiles have been measured. Left: Profile A is from the southern side of the ice stream, profile B from the center (the ice is about 2500 m thick there) and D on the northern margin. Notice the basal temperate ice at D and also at A. The very cold ice in the middle of the profiles is advected and is slowly warming up. Right: Closeup of the 31 m thick temperate layer at site D. The cold-temperate transition surface CTS is at freezing conditions. The Clausius-Clapeyron gradient (dashed line) is $\gamma = 0.0743\,\mathrm{K\,MPa^{-1}}$. From *Lüthi et al.* (2002).

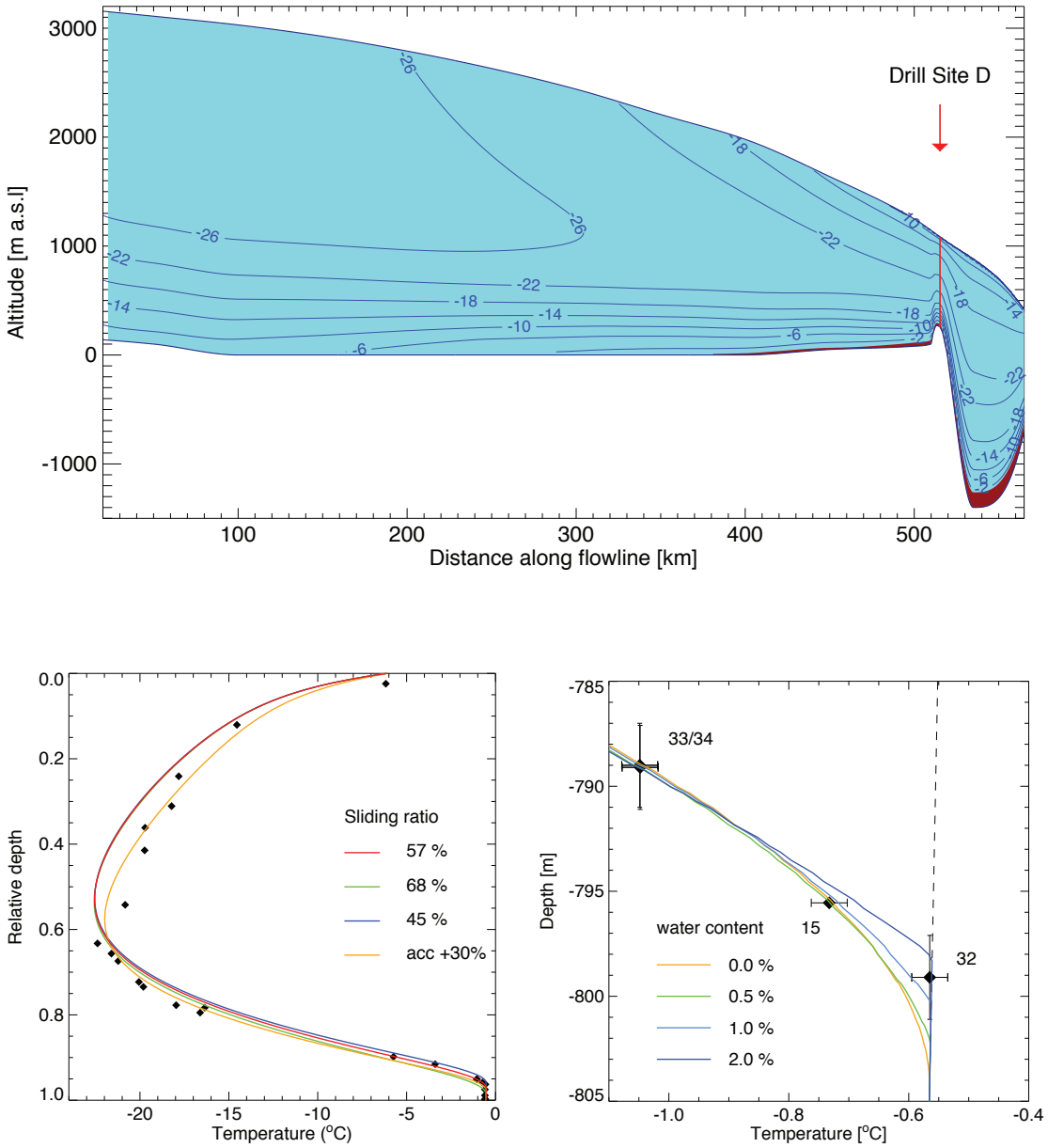

Figure 12: Top: Temperature distribution along a flow line in the Greenland Ice Sheet, and passing through drill site D. Clearly visible is the advection of cold ice and the onset of a basal temperate layer far inland at 380 km. Left: Modeled temperature profiles for different ratios of basal motion. Right: Modeled temperature profiles for different values of the water content in the temperate ice. From *Funk et al.* (1994) and *Lüthi et al.* (2002).

This heat has to be produced locally, since heat fluxes in the temperate zone below 800 m depth are downward (away from the CTS), but very small due to the Clausius-Clapeyron temperature gradient. The only way to produce this heat is by freezing the water contained within the temperate ice. From a flow model we know that the CTS moves with respect to the ice by $v_{\text{freeze}} \sim 1\,\text{m}\,\text{a}^{-1}$. With a moisture content of $\omega = 1\,\%$ (by volume) we obtain a heat production rate of

$$\begin{aligned} P = \omega\, v_{\text{freeze}}\, \rho_w L \;&\simeq\; 0.01 \cdot 1\,\text{m}\,\text{a}^{-1} \cdot 1000\,\text{kg}\,\text{m}^3 \cdot 3.33 \cdot 10^5\,\text{J}\,\text{kg}^{-1} \\ &= 3.55\,\text{MJ}\,\text{a}^{-1}\,\text{m}^{-3} \simeq 0.113\,\text{W}\,\text{m}^{-3} \end{aligned} \tag{23}$$

which matches up nicely with the heat transported away by diffusion (Eq. 22). A detailed analysis with the flow model shows that the most likely value for the water content is about 1.5 % (Fig. 12, bottom right). Another interesting result form the model is that an ice column passing through drill site D has already lost the lowest 40 m through melting at the glacier base.

5 An enthalpy formulation for glaciers and ice sheets

To model polythermal ice masses, ideally one would solve the temperature equation (Eq. 2) in cold ice and the water content equation (Eq. 18) in temperate ice, and applying Stefan-type matching conditions at the CTS. The CTS is a free boundary in such models and may be treated with front-tracking methods. Because they require an explicit representation of the CTS as a surface, however, such methods are somewhat cumbersome to implement.

Enthalpy methods describe the CTS as a level set of the enthalpy variable. No explicit surface-representation scheme is required and no *a priori* restrictions apply to CTS shape. Transitions between thermal structures caused by changing climatic conditions can be modeled even if nontrivial CTS topology arises at intermediate stages.

The specific enthalpy is often defined as $E = U + p/\rho$ where U is the specific internal energy and p is the pressure. (Note E and U have SI units $\text{J}\,\text{kg}^{-1}$.) Here we use "enthalpy" synonymous with "internal energy", $E = U$, because we do not include the work associated with changing the volume, namely the p/ρ term in the specific (per volume) case. The functional relationships between enthalpy, liquid water fraction, and temperature is given by

$$T(E,p) = \begin{cases} T_{\text{i}}(E), & E < E_{\text{s}}(p), \\ T_{\text{m}}(p), & E_{\text{s}}(p) \le E, \end{cases} \tag{24}$$

$$\omega(E,p) = \begin{cases} 0, & E < E_{\text{s}}(p), \\ L^{-1}(E - E_{\text{s}}(p)), & E_{\text{s}}(p) \le E, \end{cases} \tag{25}$$

where $E_{\text{s}}(p)$ is the enthalpy of $\omega = 0$ ice at the pressure-melting temperature $T_{\text{m}}(p)$. Schematic plots of temperature and water content as functions of enthalpy are shown

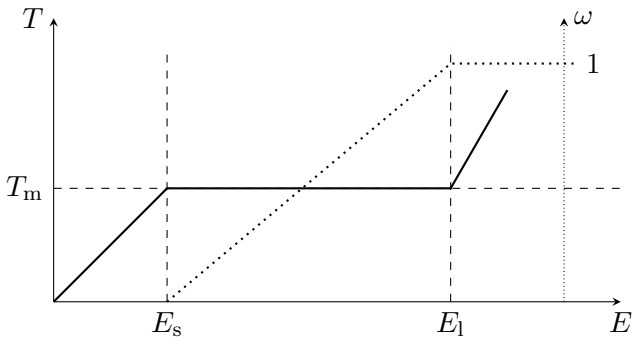

Figure 13: At fixed pressure p the temperature of the ice/liquid water mixture is a function of enthalpy, $T = T(E, p)$ (solid line), as is the liquid water fraction, $\omega = \omega(E, p)$ (dotted line). Points $E_\mathrm{s}(p)$ and $E_\mathrm{l}(p)$ are the enthalpy of pure ice and pure liquid water, respectively, at temperature $T_\mathrm{m}(p)$.

in Figure 13, with points E_s and $E_\mathrm{l}(p) = E_\mathrm{w}(T_\mathrm{m}(p), p) = E_\mathrm{s}(p) + L$ noted. Equations (24) and (25) will only be applied to cold or temperate ice (mixtures), and therefore $E < E_\mathrm{l}(p)$ in all cases.

We can then write the enthalpy balance equation as

$$\rho \left(\frac{\partial E}{\partial t} + \mathbf{v} \cdot \nabla E \right) = -\nabla \cdot \mathbf{q} + Q \tag{26}$$

with

$$\mathbf{q} = \begin{cases} -K_\mathrm{i}(E)\, \nabla E, & \text{cold}, \\ -k(E,p) \nabla T_\mathrm{m}(p) - K_0 \nabla E, & \text{temperate}, \end{cases} \tag{27}$$

where K_i and K_0 are the enthalpy diffusivity of cold and temperate ice, respectively, and k is the heat conductivity expressed in terms of enthalpy.

In writing the above enthalpy equations, we have assumed that we're dealing with incompressible ice. It is, however, important to note that the enthalpy framework is more general, and can be easily extended to the compressible case. Because the enthalpy equation is the same type of partial differential equation as the temperature equation, rendering an existing numerical model polythermal is quite straigth-forward. As so often, the devil lies in specifying the boundary conditions. For a comprehensive (and lengthy) discussion of an enthalpy formulation for glaciers and ice sheets, see *Aschwanden et al.* (2012).

Literature

Aschwanden, A., E. Bueler, C. Khroulev, and H. Blatter (2012), An enthalpy formulation for glaciers and ice sheets, *J. Glaciol.*, *58*(209), 441–457, doi:10.3189/2012JoG11J088.

Bamber, J. L. (1988), Internal reflecting layers in Spitsbergen glaciers., *Ann. Glaciol.*, *9*, 5–10.

Blatter, H. (1987), On the thermal regime of an arctic valley glacier, a study of the White Glacier, Axel Heiberg Island, N.W.T., Canada, *J. Glaciol.*, *33*, 200–211.

Blatter, H., and G. Kappenberger (1988), Mass balance and thermal regime of Laika ice cap, Coburg Island, N.W.T., Canada, *J. Glaciol.*, *34*, 102–110.

Breuer, B., M. A. Lange, and N. Blindow (2006), Sensitivity studies on model modifications to assess the dynamics of a temperate ice cap, such as that on King George Island, Antarctica, *J. Glaciol.*, *52*, 235–247.

Classen, D. F., and G. K. C. Clarke (1971), Basal hot spot on a surge type glacier, *Nature*, *229*, 481–483.

Duval, P. (1977), The role of water content on the creep rate of polycrystalline ice, in *Isotopes and impurities in snow and ice*, pp. 29–33.

Eisen, O., M. P. Lüthi, P. Riesen, and M. Funk (2009), Deducing the thermal structure in the tongue of Gornergletscher, Switzerland, from radar surveys and borehole measurements., *Ann. Glaciol.*, *50*(51), 63–70.

Fountain, A. G., and J. S. Walder (1998), Water flow through temperate glaciers, *Reviews of Geophysics*, *36*, 299–328.

Fountain, A. G., R. W. Jacobel, R. Schlichting, and P. Jansson (2005), Fractures as the main pathways of water flow in temperate glaciers., *Nature*, *433*, 618–621.

Funk, M., K. Echelmeyer, and A. Iken (1994), Mechanisms of fast flow in Jakobshavns Isbrae, Greenland; Part II: Modeling of englacial temperatures, *J. Glaciol.*, *40*, 569–585.

Greve, R., and H. Blatter (2009), *Dynamics of Ice Sheets and Glaciers*, Advances in Geophysical and Enviornmental Mechanics and Mathematics, Springer Verlag.

Gusmeroli, A., T. Murray, P. Jansson, R. Pettersson, A. Aschwanden, and A. D. Booth (2010), Vertical distribution of water within the polythermal Storglaciären, Sweden, *J. Geophys. Res.*, *in press*.

Harrison, W. D. (1975), Temperature measurements in a temperate glacier, *J. Glaciol.*, *14*, 23–30.

Holmlund, P., and M. Eriksson (1989), The cold surface layer on Storglaciären., *Geographiska Annaler*, *71A*, 241–244.

Iken, A., K. Echelmeyer, M. Funk, and W. D. Harrison (1993), Mechanisms of fast flow in Jakobshavns Isbrae, Greenland, Part I: Measurements of temperature and water level in deep boreholes, *J. Glaciol.*, *39*, 15–25.

Jania, J., D. Mochnacki, and B. Gadek (1996), The thermal structure of Hansbreen, a tidewater glacier in southern Spitsbergen, Svalbard, *Polar Research*, *15*, 53–66.

Lliboutry, L. A. (1976), Physical processes in temperate glaciers, *J. Glaciol.*, *16*, 151–158.

Lüthi, M. P., and M. Funk (2001), Modelling heat flow in a cold, high altitude glacier: interpretation of measurements from Colle Gnifetti, Swiss Alps, *J. Glaciol.*, *47*, 314–324.

Lüthi, M. P., M. Funk, A. Iken, M. Truffer, and S. Gogineni (2002), Mechanisms of fast ow in Jakobshavns Isbræ, Greenland, Part III: measurements of ice deformation, temperature and cross-borehole conductivity in boreholes to the bedrock, *J. Glaciol.*, *48*(162), 369–385.

Mader, H. M. (1992), Observations of the water-vein system in polycrystalline ice, *J. Glaciol.*, *38*(130), 333–347.

Nye, J. F. (1989), The geometry of water veins and nodes in polycrystalline ice, *J. Glaciol.*, *35*(119), 17–22.

Paterson, W. S. B. (1971), Temperature measurements in Athabasca Glacier, Alberta, Canada, *J. Glaciol.*, *10*, 339–349.

Paterson, W. S. B. (1994), *The Physics of Glaciers*, 480 pp., Pergamon, New York.

Pettersson, R., P. Jansson, and H. Blatter (2004), Spatial variability in water content at the cold-temperate transition surface of the polythermal Storglaciären, Sweden., *J. Geophys. Res.*, *109*(F2), 1–12, doi:10.1029/2003JF000110.

Raymond, C. F., and W. D. Harrison (1975), Some observations on the behaviour of the liquid and gas phases in temperate glacier ice, *J. Glaciol.*, *14*, 213–233.

Ritz, C. (1987), Time dependent boundary conditions for calculation of temperature fields in ice sheets, in *The Physical Basis of Ice Sheet {M}odelling*, vol. 170, pp. 207–216, Vancouver.

Ryser, C. (2009), The polythermal structure of Grenzgletscher, Valais, Switzerland, Master thesis, ETH Zurich.